Local identification of groundwater dependent vegetation using high-resolution Sentinel-2 data – A Mediterranean case study

Léonard El-Hokayem [a,c,*], Pantaleone De Vita [b], Christopher Conrad [a,c]

[a] Institute of Geosciences and Geography, Martin Luther University Halle-Wittenberg, Halle (Saale) 06120, Germany
[b] Department of Earth, Environmental and Resources Sciences, University of Naples Federico II, Naples 80126, Italy
[c] German Centre for Integrative Biodiversity Research (iDiv) Halle-Jena-Leipzig, Leipzig 04103, Germany

ABSTRACT

Groundwater dependent ecosystems (GDEs) are biodiversity hotspots and provide important ecosystem services. This study presents a novel multi-instrument concept for the local identification of groundwater dependent vegetation (GDV) in the Mediterranean. The concept integrates high-resolution Sentinel-2 remote sensing data with available geodata and requires in situ vegetation data for validation and calibration. The approach combines five criteria to identify GDV: 1) high vitality, and wetness during dry period, 2) low seasonal changes in vitality and leaf area, 3) low interannual changes in vitality, 4) high topographic potential of water accumulation and low water table depth, 5) high potential inflow dependency. Iso Cluster Unsupervised Classification (ICUC) was applied to identify GDV in the study area (Campania, Italy). Botanical field mapping was utilized for validating the remote sensing approach, as it exhibited significant differences between GDV and Non-GDV in terms of ecohydrological indicator values, leaf anatomy and phreatophyte coverage. According to a new simple ecohydrological rule set that considers phreatophyte cover and mean moisture value of non-phreatophyte species, 9% of vegetation plots are considered GDV and 33% likely GDV. 80% of all GDV derived from classification occur in hydrostratigraphic units (HSU) that are characterized by surficial groundwater circulation and low permeability. The overall accuracy of classifying likelihoods is 62.7%. For 14.6% of the plots, non-GDVs were classified as GDVs (false positives), and only one GDV plot has been classified falsely as non-GDV (false negative). Local results on GDV locations can be overlaid with aquifer use or aquifer reaction to climate change in order to identify GDV under threat and implement sustainable managements of groundwater resources.

1. Introduction

Groundwater plays an important role as a resource for terrestrial vegetation. Evaristo & McDonnell (2017) showed in a global stable isotope *meta*-analysis that the prevalence of groundwater use in Mediterranean forests, woodlands and scrubs is 50 %. Accordingly, a variety of ecosystems require the presence or the contribution of groundwater to maintain their ecological function, composition, or structure and are groundwater dependent ecosystems (GDEs) (Eamus et al., 2006). Temporal and spatial variability of the groundwater flow associated with geology, climate and land use influences the presence and characteristics of GDEs. These influencing variables show that GDEs are exposed to several anthropogenic threats, including overexploitation, pollution, or climate change (Eamus et al., 2015). Subsequently, ecosystem functions and biodiversity are at risk. As future climate predictions in the

Mediterranean assume an overall decrease in precipitation, significant warming and drying in summer, decrease in runoff and aquifer recharge is to be expected (Tuel & Eltahir, 2020). Altogether, trends in climate and land use change aggravate the situation and may also endanger GDE in places where low human pressure currently exists. Nevertheless, tackling these threats is of paramount importance to maintain related ecosystem services, e.g., climate regulation, water storage or soil development (EC, 2007) and requires improving the high-resolution, local, on-the-ground identification of GDEs.

In general, identification of groundwater dependent vegetation (GDV) relies on the usage of several direct and indirect methods. Direct methods include botanical observations, as well as determination of hydrogeological parameters. The vegetative approach relies on mapping of phreatophytes, groundwater dependent habitats or indicator plants (e.g., Killroy et al., 2008). Methods aiming for hydrological parameters

comprise fluctuation in groundwater depth, identification of water sources from stable isotopes, geological mapping or groundwater sampling (e.g., Hoogland et al., 2010; Jones et al., 2020; Killroy et al., 2008). These ground-based measurements are only suitable for small areas as data acquisition is often selective, time and labour-consuming, and highly dependent on expert knowledge (Doody et al., 2017). On the other hand, these methods are most likely very accurate and reliable when it comes to assessing veritable groundwater dependency. Indirect methods to locate GDV integrate remote sensing with other geodata and have gained importance in recent years (Eamus et al., 2016). In particular, increased availability in remote sensing and other geodata opens up alternative strategies to map GDV at larger scales (Pérez Hoyos et al., 2016). Indirect GDV identification allows covering larger areas at a relatively lower cost even though processing of the data is time and CPU intensive.

Major limitation of local identification of GDV using remote sensing techniques relies on the restricted spatial resolution of datasets used to date (Landsat 25–30 m, MODIS 250 m) (e.g., Box et al., 2022; Doody et al., 2017; Gou et al., 2015; Páscoa et al., 2020). This causes GDVs with a small spatial extent to be underrepresented in general. In recent GDV studies, indicators relaying on spectral vegetation indices as well as topographical analyses of digital elevation models (DEM), Water table depth (WTD) and climate data (precipitation, evapotranspiration) form common criteria applied to address for delineation of GDV (e.g., Doody et al., 2017; Gou et al., 2015; Münch & Conrad, 2007). However, a combined framework, making use of these different input variables is still missing, but holds the possibility to improve classification results.

Furthermore, field investigations are required as they ensure to ground truth the occurrence of possible GDV. Such campaigns often require specialized equipment that may not be available in certain cases (Jones et al., 2020). However, in situ validation of the results and further calibration concerning pixel-wise classification of GDV is still the exception in remote sensing approaches (Pérez Hoyos et al., 2016). Rather, existing maps referring to vegetation patterns, land cover and WTD or expert opinion have been utilized for validation so far. For example, Münch & Conrad (2007) validated GDEs in the Sandveld region in South Africa using the extent of wetland-riverine footprints and occurrence of groundwater dependent indicator species. A study in Texas (USA) got verified using existing maps of phreatophytes and wetlands (Gou et al., 2015). Páscoa et al. (2020) assessed the quality of a GDV classification in the Iberian Peninsula with WTD and land cover types.

This study will focus on GDV (terrestrial vegetation reliant on subsurface availability of groundwater (Eamus et al., 2006) in the Mediterranean that is, inter alia, formed by phreatophytes (Meinzer, 1927). For this purpose, a novel designed remote sensing framework combining several indicator groups that showed high potential in recent approaches targeting the identification of GDV will be tested locally. In addition, the need for in situ validation is demonstrated and implemented through a rather simple, easy-to-reproduce botanical field campaign. Ideally, the framework should be applicable also to larger scales by simply changing input data sources.

Firstly, different criteria applied in several local to regional approaches to map GDV in semi-arid areas are combined in a novel mapping framework. Vegetative (temporal signals of plant vitality), hydrogeologic (accumulation of water) and climatic criteria (precipitation, evapotranspiration) will be merged together in a concept for mapping GDV by the use of remote sensing techniques and geodata integration. In order to overcome limitations of spatial resolution, the usage of spatial and temporal high-resolution (10 m, 5-day) Sentinel2 (S2) data displays a novelty in the identification of GDV. Spectral indices (e.g., Enhanced Vegetation Index (EVI)) or biophysical parameters (Leaf Area Index (LAI)) that have been underexplored but show high potential for GDV detection will be included. The application of hybrid classification (Iso Cluster Unsupervised Classification (ICUC) in terms of GDV mapping was tested for the first time. Moreover, the usage of in situ

botanical data in order to validate results and optimize class boundaries between GDV likelihoods displays a novelty.

The mapping concept is initially designed, tested, and validated in a Mediterranean study area located in the 'Cilento, Vallo di Diano and Alburni National Park' in South Italy. For the period from 2017 to 2021 a total of 102 S2-scences was analysed in terms of temporal variability of spectral signals targeting plant vitality and moisture. Moreover, 116 comprehensive vegetation surveys and 100 comparative measurements of leaf chlorophyll content using the Soil Plant Analysis Development value (SPAD) were recorded and analysed. SPAD measurements address for in situ differences of photosynthetic activity between co-occurring *Quercus* species in GDV and non-GDV.

As groundwater in arid and semi-arid regions plays a key role in providing drinking water, supporting irrigated agriculture and, sustaining important terrestrial ecosystems, a local GDV mapping framework for the Mediterranean biome will be an important tool in order to identify and study vegetation reliant on groundwater, which may in turn support decisions on groundwater abstraction in order to protect these hotspots of biodiversity.

2. Study area

The study area is located in southern Italy (Campania region) inside the 'Cilento, Vallo di Diano and Alburni National Park' (Fig. 1).

The area was chosen due to its relative homogeneity in climate, vegetation, soil, geology and hydrogeology, and its heterogeneity in WTD and high naturalness in terms of land cover. Such factors were considered favourable to recognize differences in vegetation predominantly induced by the presence of groundwater. According to Köppen and Geiger classification (Beck et al., 2018) the area belongs to the hot-summer Mediterranean climate (Csa) with a distinction between a cold-wet season from October till March and a hot-dry season from April till September (Romano et al., 2018). The vegetation in the study area is mainly characterized by broadleaved deciduous or evergreen forests and Mediterranean scrub (European Environment Agency (EEA), 2017). Typical GDV in the area of interest (AOI) is associated with Mediterranean riparian forests and thermophilous deciduous oak forests, as well as evergreen holm oak forests. Non-groundwater dependent scrubs mostly belong to the class of Mediterranean maquis and arborescent matorral including brushes, thickets and heath-garrigues. Most important phreatophytes in the area include:

Q. pubescens, Q. ilex, Salix alba, Phragmites australis, Alnus cordata, Sambucus nigra, Q. cerris, Populus nigra. Information on rooting depth was not available for the AOI.

At local scale, five hydrostratigraphic units (HSU) (Maxey, 1964) with different modes of groundwater circulation can be distinguished (Casciello et al., 1995): 1) arenaceous-marly-clayey complex, 2) marly-clayey complex, 3) arenaceous-conglomeratic complex 4) detrital complex and 5) alluvial complex. Processes of infiltration and underground water circulation in the AOI are strongly related to the presence of fine-grained interbed layers and fracturing. The arenaceous-marly-clayey complex shows alternating permeability from arenaceous rocky beds, permeable for fracturing, and pelitic interlayers with low permeability due to porosity. The occurrence of pelitic interlayers defines an overall low degree of permeability by porosity and fracturing, which results in a scarce and surficial groundwater circulation occurring mainly into the more permeable weathering, or regolith, zone (Selby, 1993) and reliant on topographic gradient. The marly-calcareous complex includes two carbonate turbidite megastrata which are moderately permeable through fracturing and, subordinately, through porosity. The degree of deepening of the water circulation appears to be rather shallow. The arenaceous-conglomeratic complex favours a medium to high degree of permeability by fracturing and porosity, which makes it the most important aquifer in the area. Underground water circulation appears deeper than in the other complexes and is oriented towards the northern part of the relief and terminating in the main springs of the area
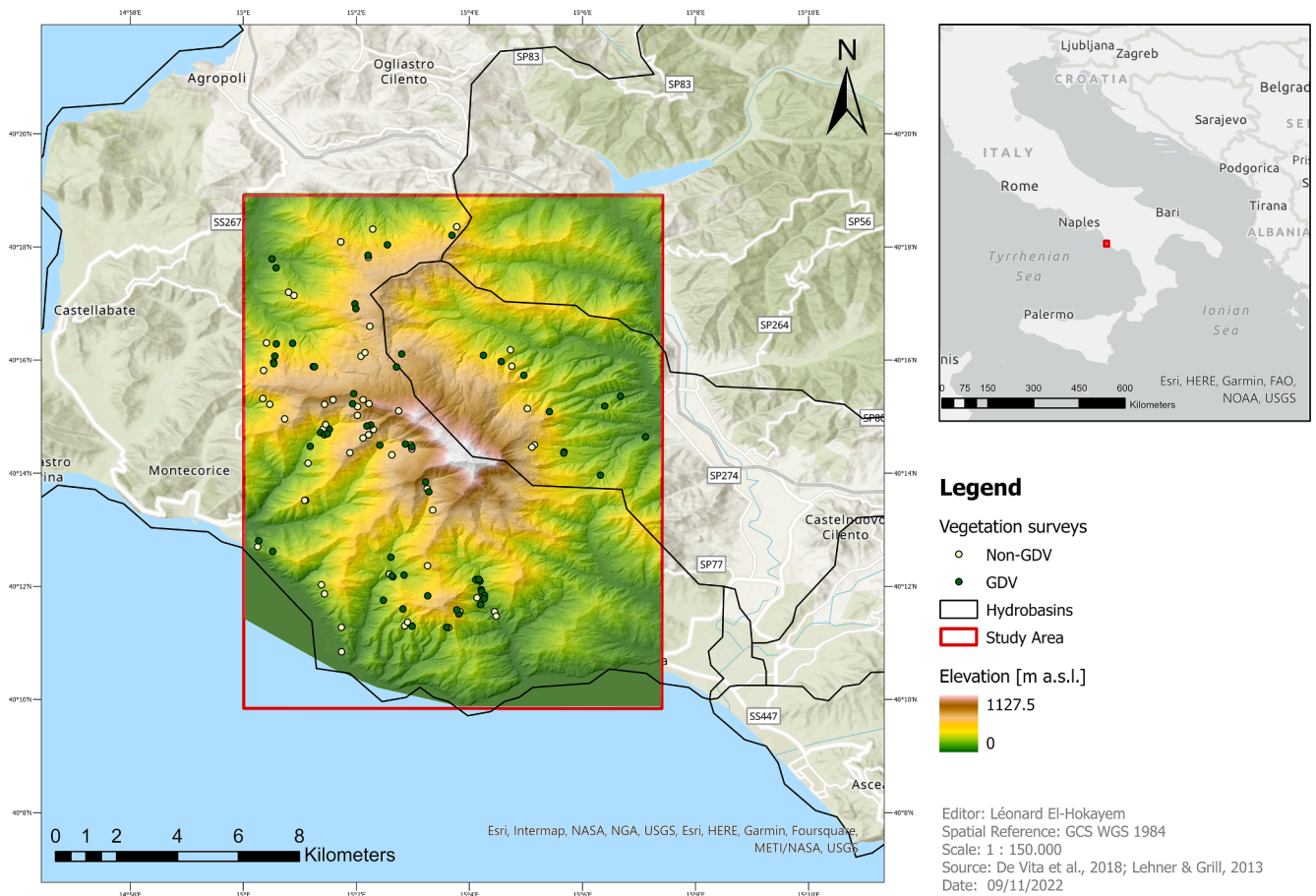
Fig. 1. Overview map of the study area 'Mount della Stella (1,130 m)', Italy with centroids at 15.06192 °E and 40.23961 °N and an area of 176 km2, 1:150,000.

(Casciello et al., 1995).

3. Material and methods

The workflow to detect GDV comprises three basic steps including 1) definition and 2) implementation of the framework, and 3) validation and calibration using ground-based data from botanical field mapping as well as landcover and hydrogeology data. The subchapters of this sections are structured accordingly. All datasets used in this study are listed in Table 1.
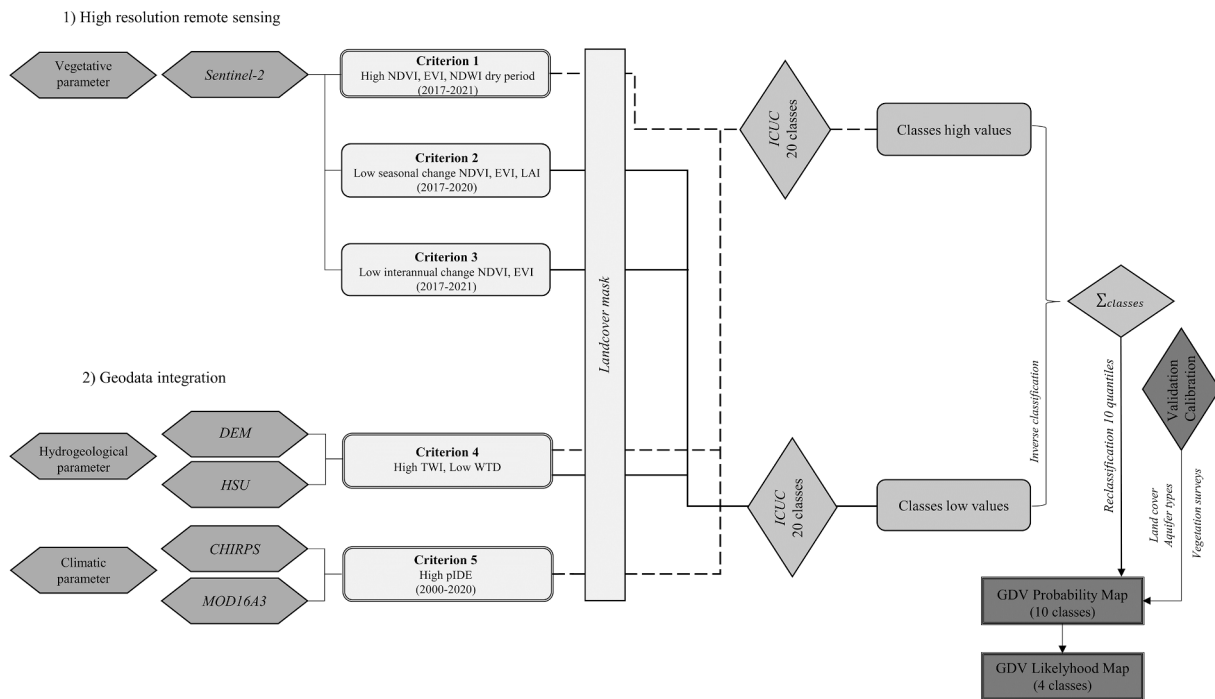
3.1. Definition of the GDV mapping framework

Underlying key concept for mapping GDV in arid and semi-arid regions is the measurement of vegetation and moisture response at the surface within an extended dry period (Barron et al., 2014). In this local approach, the dry period of the AOI was derived from literature (Romano et al., 2018).

The framework (Fig. 2) combines analyses on high-resolution remote sensing data and existing geodata. Three main parameters (vegetative, hydrogeological, and climatic) are defined by a total of five criteria which consist of specific indicators respectively. Hence, the approach includes the derivation of remote sensing indices and biophysical parameters to determine vegetation status and vitality (e.g., Barron et al.,

Table 1
Compilation of datasets used for classification and validation.

Dataset	Application	Temporal resolution	Spatial resolution	Unit	Period	Data Source
Campanian's aquifers	Water table depth, HSU	–	200 m	m; mm; -	–	De Vita et al., 2018
CHIRPS	Local precipitation data	Yearly	0.05° (~4.3 km at 40 N)	mm	2000–2020	Funk et al., 2015
DEM	Calculation of Topographic Wetness Index (TWI)	–	5 m	m	–	Regione Campania, 2004
Europe Land Cover Map	Masking of the input data	2017	10 m	–	2017	Malinowski et al., 2020
MOD16A3	Total evapotranspiration	Yearly	500 m	kg/m^2/8day	2000–2020	Running et al., 2017
Sentinel-2	Biogeophysical parameters and vegetation indices	5-Day	10 m	–	2017–2021	ESA, 2021
Soil Plant Analysis Development value (SPAD)	Photosynthetic activity	2021	–	SPAD	2021	This study
Vegetation surveys	Plant traits, phreatophyte coverage	2021	10 m	–	2021	This study

Fig. 2. Framework for GDV mapping in the Mediterranean biome and implementation for the AOI using certain vegetation indices (Normalized Difference Vegetation Index (NDVI), Normalized Difference Water Index (NDWI), EVI) and a biophysical parameter (LAI) derived from S2- data (10 m) from 2017 to 2021, a local DEM (5 m), a dataset about HSU in Campania (De Vita et al., 2018), global CHIRPS precipitation data (0.05°) and the MOD16A3 product on evapotranspiration (500 m). The framework can be implemented for different Mediterranean AOI at local scale also by adapting datasets and the indicators for the criteria.

2014; Doody et al., 2017; Gou et al., 2015; Lv et al., 2012), analyses on DEM such as TWI (Münch & Conrad, 2007), spatial variations in WTD (Marínez-Santos et al., 2021), as well as climatic variables for precipitation and evapotranspiration (Doody et al., 2017).

The five criteria were joined in a novel rule set, including indicators that were already tested in the mentionend studies on GDEs. Criteria 1–3 aggregate indicators on vegetative analysis of high-resolution satellite imagery using multiple spectral bands and indices together with timeseries (Pasquarella et al., 2016). Criterion 4 and 5 target hydrogeology and climate. The first criterion aims at the identification of areas that remain green or wet during the dry period (Eamus et al., 2016). Criterion 2 includes vegetation which exhibits low seasonal changes in leaf area or vitality. Criterion 3 permits the localization of vegetation with low interannual variability in greenness and activity (Gou et al., 2015). Criterion 4 includes hydrogeological parameters, especially indicating areas where water accumulation takes places (Münch & Conrad, 2007) and WTD is low (Marínez-Santos et al., 2021). For criterion 5, the potential inflow dependency (pIDE) of pixels was used to integrate climate data (Doody et al., 2017). At the time of analysis, annual means for criteria 2 and 5 were not available for 2021 yet. In order to connect the different indicators and criteria, pixel-wise hybrid classification was performed using Iso Cluster Unsupervised Classification (ICUC) since no information on GDV in the study area was available before. The classes got translated to ten GDV probability classes, which were finally subdivided in GDV likelihoods by means of an independent ecological rule set using vegetation data collected during the botanical field campaign.

3.2. Implementation

3.2.1. Criteria 1–3 (based on high-resolution remote sensing)

The proposed workflow for detecting GDV in the Mediterranean biome was tested in the study area using S2- surface reflectance data from 2017 to 2021. In total 102 S2-scenes with a maximal cloud cover of 20 % and a resolution of 10 m were downloaded and pre-processed using the 'sen2r' R-package (Ranghetti et al., 2020).

Spectral vegetation indices from remote sensing hold an enormous benefit in the assessment of vegetation biomass, water use, plant stress or plant health and further in the identification of GDV through analyses of distribution and temporal trends. As plant density is often correlated with water availability in arid and semi-arid environments (Eamus et al., 2015), a key conceptual model for delineating the location of GDV is the identification of 'green islands' (Akasheh et al., 2008). Three multispectral indices: NDVI (Rouse et al., 1974), EVI (Huete et al., 2002) and NDWI (Gao, 1996) that also found application in recent studies (Box et al., 2022) were useful for indirect evaluation of greenness, wetness and stress of surface conditions to derive potential GDV locations. The indices were calculated following equation ((1)–(3)): $NDVI = \frac{(\rho NIR - \rho Red)}{(\rho NIR + \rho Red)}$ (1)

where ρNIR represents the reflectance in the near-infrared and ρRed is the reflectance in the red visible band.

$$EVI = G* \frac{(\rho NIR - \rho Red)}{(\rho NIR + C_1 * \rho Red - C_2 * \rho Blue + L)} \quad (2)$$

where ρBlue is the reflectance in the blue band and C1 and C2 are aerosol resistance coefficients. G represents a gain factor, and L is the canopy background. In the MODIS-EVI algorithm the coefficients are defined as: L = 1, C1 = 6, C2 = 7.5 and G = 2.5.

$$NDWI = \frac{(\rho NIR - \rho MIR)}{(\rho NIR + \rho MIR)} \quad (3)$$

where ρMIR represents the reflectance in the short-wave infrared band.

LAI was calculated by following equation (4) using ESA's SentiNel Application Platform (SNAP) (Weiss & Baret, 2016).

$$LAI = \frac{0.5 * AVeg}{AGround} \quad (4)$$

where A_{Veg} is the area of photosynthetically active elements of the vegetation and A_{Ground} as the horizontal ground area.

Criterion 1 assumes that limited precipitation over an extended dry period of five months leads to depleted soil moisture stores in general. Data was obtained two months after onset of the dry period (July) until the beginning of the wet period (end of September) for the years 2017–2021. Consequently, vegetation that is able to maintain a constant vitality and wetness as well as high density (Lv et al., 2012) during this period is likely to use groundwater. This criterion is susceptible to vegetation found on deep soils with a high water holding capacity and lower soil water deficit, regardless arid conditions in summer. Moreover, species that are evergreen or well adapted to drought could show spectral signals similar to the ones postulated for GDV without actually using groundwater. Mean raster values were calculated for NDVI, EVI, NDWI for each dry period from 2017 to 2021 (criterion 1). To meet criterion 2 (vegetation shows low seasonal changes in LAI), annual standard deviation of LAI, NDVI and EVI were calculated for 2017–2020 in order to assess vegetation structure and function across contrasting seasons (wet and dry) (Eamus et al., 2016). Nevertheless, differences in phenology (evergreen vegetation shows consistent greenness throughout the year, while deciduous vegetation have a high alteration in LAI) could confound the classification here. In order to overcome limitations of criteria 1 and 2 another criterion was introduced by Tweed et al. (2007) that aims for vegetation showing low interannual variability in activity. It is considered that GDV shows similar signals in particular dry and wet years due to the existence of an external groundwater source. For criterion 3, NDVI and EVI standard deviation were calculated for the mean values of the dry periods from 2017 to 2021 which could be influenced e.g., by changes in landcover.

3.2.2. Criteria 4 and 5 (based on geodata products)

The implementation of the criteria 4 and 5 was based on a 5 m-DEM derived by the regional vector topographic map (1:5,000) (Regione Campania, 2004) and mean annual precipitation data derived from CHIRPS (0.05°) and the MOD16A3 (500 m) product. WTD (200 m) in the study area was derived from De Vita et al. (2018). Landscape wetness potential and water accumulation based on topographical features are strongly related to possible locations of GDV (Münch & Conrad, 2007). TWI was calculated from the local DEM to quantify topographic control on hydrological processes:

$$TWI = \ln\left(\frac{As}{\tan\beta}\right) \tag{5}$$

where, As is the specific catchment area (the cumulative upslope area draining through a cell divided by the contour width) and β is the local slope angle, giving a hint to long-term soil moisture availability (Beven & Kirkby, 1979). TWI was calculated by means of the 'Topographic Wetness Index' tool in QGis 3.12 using the standard method including slope and catchment area. Besides TWI, criterion 4 also included water table depth as additional indicator (De Vita et al., 2018).

pIDE (criterion 5) was displayed as simple ratio between mean evapotranspiration and mean precipitation for 2000–2019 pixel-wise in order to highlight areas where climatic conditions indicate external water inflow (Doody et al., 2017). Vegetation pixels showing higher annual evapotranspiration rates than actual precipitation are hence more likely to be groundwater dependent.

In summary, rules for classifying vegetation pixels to be groundwater dependent include: 1) high vitality or moisture during dry periods, 2) low seasonal variability in vitality, 3) low interannual changes in vitality, 4) shallow groundwater and topographical conditions favouring water accumulation and 5) annual evapotranspiration exceeding precipitation.

3.2.3. Classification

In order to only process the most natural vegetation, a mask was created based on the "European Landcover Map" (accuracy = 86 %) (Malinowski et al., 2020). Therefore, all pixels representing: clouds, artificial surfaces and constructions, cultivated areas, vineyards and water bodies were excluded, reducing the area by 13 %. Finally, all input raster data were harmonized in terms of extent (AOI), resolution (10 m) and projection (WGS 1984, UTM zone 33 N) by means of the *spatial_sync_raster* function in the R-package 'spatial.tools' using nearest neighbour interpolation (Greenberg, 2020). Finally, all rasters were masked against the land cover mask.

The identification of GDV is provided by hybrid classification. Firstly, an unsupervised classification is performed that does not need training sets, as it attempts to find underlying structures automatically via common spectral characteristics, and groups pixels that are statistically similar, into a specified number of classes (Duda & Canty, 2002). Afterwards, the images are reclassified by running a supervised classification using the statistics of the unsupervised classification as training knowledge (Al-doski et al., 2013). The utilized ICUC tool performs the classification based on a series of input raster bands by a combination of Iso Cluster and Maximum Likelihood classification (ESRI, 2021). Equation (6) shows the underlying algorithm:

$$Z = \frac{(X - O_{min}) * (N_{max} - N_{min})}{(O_{max} - O_{min}) + N_{min}} + N_{min} \tag{6}$$

where Z is the output raster with new data ranges, X is the input raster, O represents the minimum or maximum value of the input raster and N is the desired minimum or maximum value for the output raster. By implementing iterative clustering, the tool first identifies natural groupings of pixels that are later used as input for the maximum likelihood tool (Green & Cooper, 2016).

In accordance with Barron et al. (2012), 20 classes were defined to consider variability of relevant land cover (n = 6), hydrogeological systems (n = 6), elevation (0–1,200 m) and soil types (n = 5) in the AOI and also allow for higher flexibility when grouping classes. The minimum class size was set 10 times higher than the number of input raster bands (ESRI, 2021). Since the algorithm uses minimum and maximum values for classification, two parallel classification runs were implemented, combining criteria where low values represent GDV and vice versa.

The assigned values from both classification runs were summed pixel-wise, to pinpoint pixels that show highest values for most criteria and hence hint to possible GDV locations. The summarized raster images with values ranging between 3 and 40 were reclassified to ten quantiles which are considered to represent the probability (0–100 %) of each pixel being groundwater dependent.

3.3. Botanical field mapping and validation

By observing patterns in range and behaviour of indicator communities or species, botanical field mapping serves as validation of the GDV-map. Further, results were used to derive class boundaries for GDV likelihoods.

A total of 116 vegetation surveys and 100 SPAD measurements were conducted in the study area. Based on the GDV probability map (ten classes) and according to recent results from other GDV studies in semi-arid environments (Doody et al., 2017; Gou et al., 2015; Páscoa et al., 2020) the area got subdivided in two main classes (Non-GDV = lower 70 %, GDV = upper 30 %). For each class, 58 vegetation surveys and 50 SPAD measurements were recorded.

Every vegetation survey contains information on: date, location, elevation, HSU, habitat, species number, stratification (tree 1 & 2, shrub, herb) and occurrence of above-ground water. For each species in the 100 m^2 plots, different plant traits (Ellenberg indicator values, plant life form, leaf anatomy) were assigned from literature respectively (Pignatti, 1982; Pignatti et al., 2005) and means were calculated plot-wise. In particular the Ellenberg indicator values allow to easily characterize

ecological conditions of plant communities in terms of light availability (L), temperature (T), continentality (K), moisture (F), soil reaction (R) and nutrients (N) (Ellenberg, 1974) which are practical to characterize groundwater dependency (Killroy et al., 2008). Furthermore, each species was classified as phreatophyte or not using different studies of phreatophyte species (e.g., Gomes Marques et al., 2019; Thomas, 2014).

Additionally, in situ reference measurements of relative leaf chlorophyll content were conducted for two co-occurring *Quercus* species in areas prior labelled GDV or non-GDV using the 'SPAD-502Plus' optical chlorophyll absorbance meter. SPAD values help to address differences in photosynthetic potential, vitality or primary production of the respective species (Richardson et al., 2002).

In a first step, all vegetation plots and SPAD sites were labelled as GDV or non-GDV according to their position on the probability map. To check whether differences in classification were reflected in actual vegetation cover, a statistical analysis of differences in plant characteristics and SPAD between these two groups was carried out. Since none of the parameters were normally distributed and the samples were independent, a Wilcoxon rank-sum test was performed for each plant trait (Traxler, 1997) (Figs. 3-4).

In a second step, the field plots were classified independently of the probability map based on an ecohydrological rule set including phreatophyte coverage (P%) and mean moisture value (F) of non-phreatophyte species. Since, no information on rooting depth of species, WTD or actual groundwater uptake was available in the field, these simple indicators help to classify GDV. A statistical approach was used to evaluate GDV classes based on phreatophyte cover using quantiles, as no thresholds are available in the literature. Following likelihoods are proposed: 1) Non-GDV (P% < 25, F < 3 (arid)), 2) Unlikely GDV (P% = 25–50, F = 3), 3) Likely GDV (P% = 50–75, F = 4) and 4) GDV (P% =

75–100, F > 4 (well supplied with water)). Based on their occurrence frequency, GDV likelihoods were transferred to the probability map, to calibrate class boundaries and test accuracy of the classification.

4. Results

4.1. Vegetation surveys

Variances between vegetation surveys can be used as on-ground confidence building for the decision whether vegetation is groundwater dependent or not. Differences between map-labelled GDV and non-GDV-plots are visible in the stratification. For GDV, tree layer 1 dominates with a mean share of 65 %. Within non-GDV the most important layer are shrubs with 76 %. Ellenberg indicator values, leaf anatomy, species richness and proportion of phreatophytes are examined for significant differences between both classes. Median indicator values (Fig. 3) in GDV account for semi-shade plants (L = 5.3), found on dry places and soils supplied with water (F = 3.9) as well as on humified soils (N = 4.6) in mesophilic or mildly basic environments (R = 5.8). Within non-GDV full sun or reduced light conditions (L = 7.9) prevail. The identified species are indicators of aridity (F = 2.9), found on nutrient-poor soils (N = 3.6) in neutral conditions (R = 5.2). According to the Wilcoxon rank-sum test, differences for indicator values were found to be highly significant (p < 0.001).

Very significant differences (p < 0.01) between both systems were found for plant life forms. Therophytes and hemicryptophytes are more likely to occur in non-GDV, while nanophanerophytes are more frequent in GDV. As for variances in leaf anatomy, higher coverage of scleromorphic species indicates non-GDV, whereas mesomorphic as well as hygromorphic species are found more often in GDV. Results of the
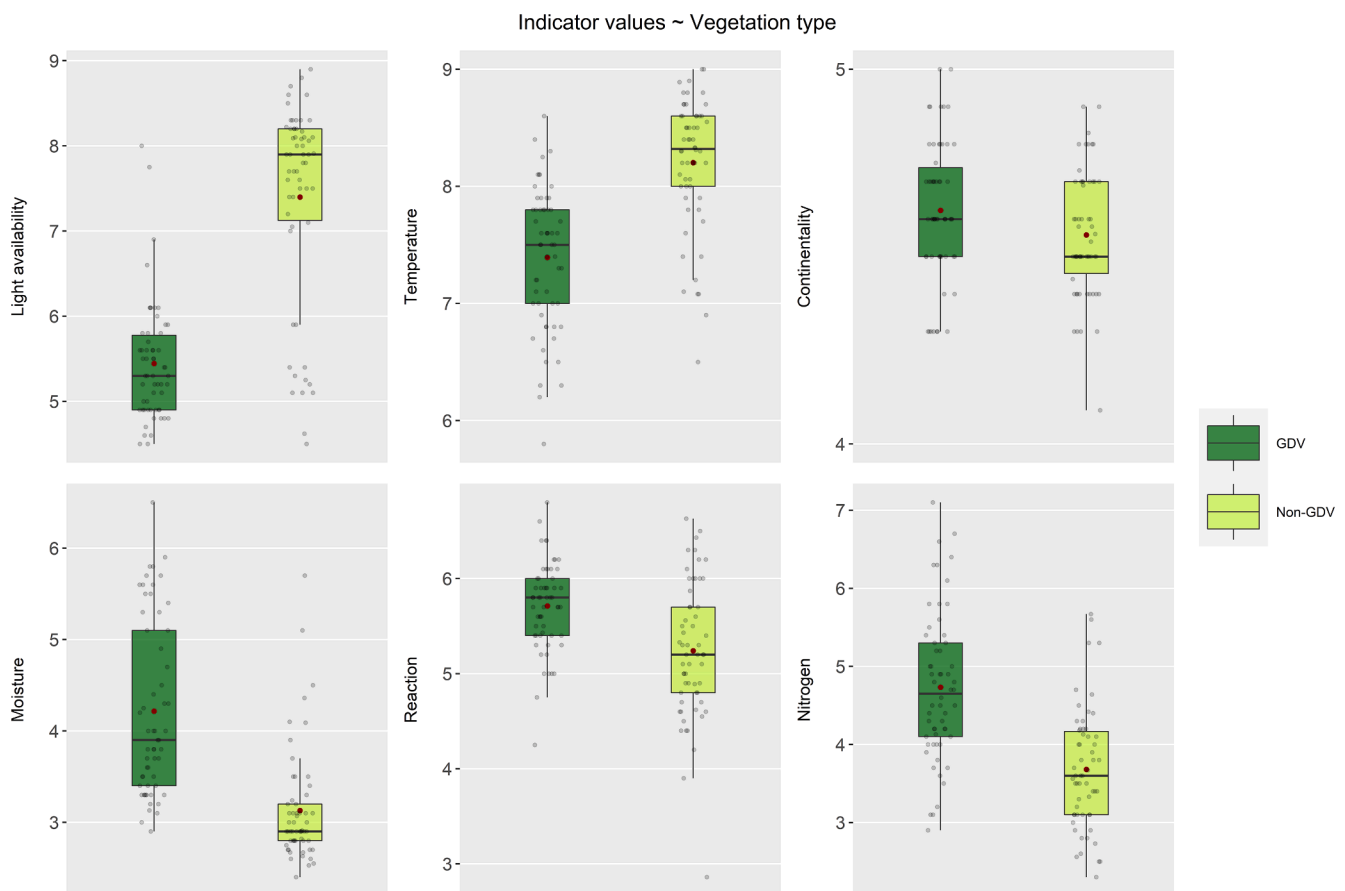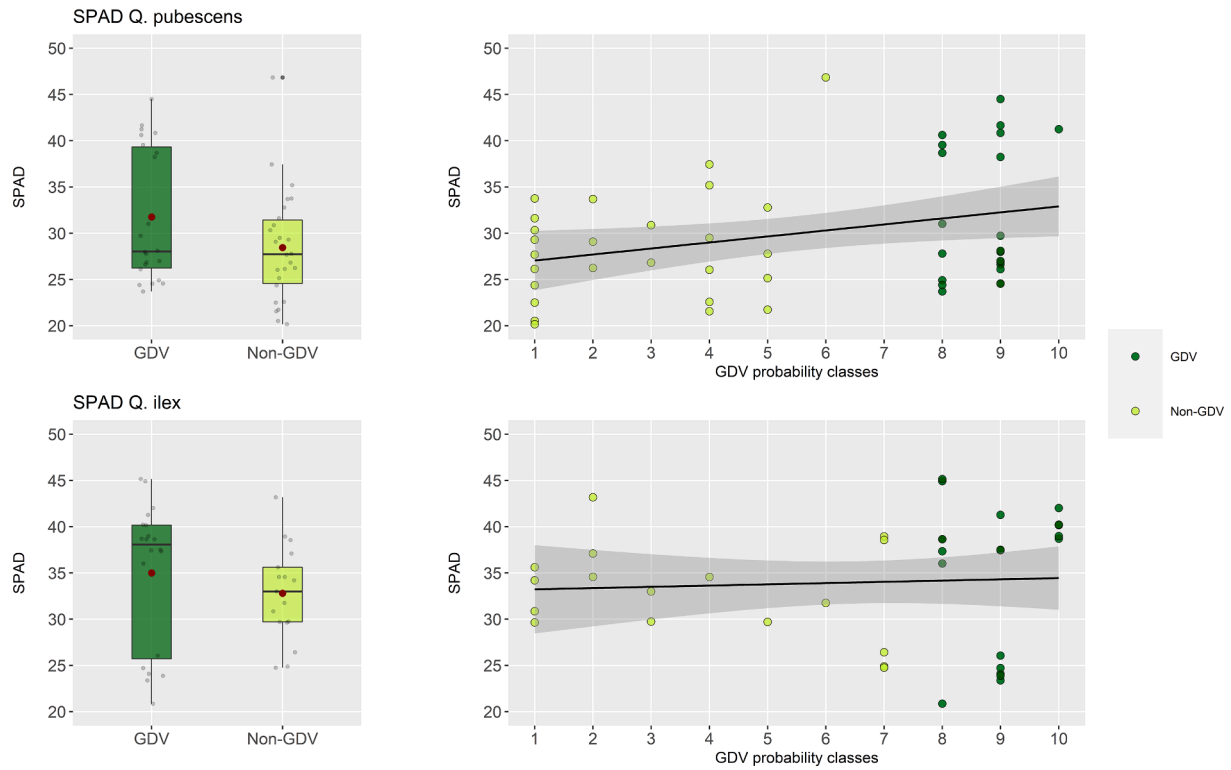

Fig. 3. Distribution of Ellenberg indicator values (L, T, K, F, R, N) in GDV and Non-GDV plots. Grey dots show the actual data points (n = 58 per class) and red dots display the mean values. Ranges are different for each value (see Pignatti et al., 2005) Differences are highly significant (p < 0.001).

SPAD values Quercus species ~ Vegetation type

Fig. 4. Distribution of SPAD values for *Q. pubescens* and *Q. ilex* between GDV and non-GDV plots and depending on GDV probability classes (1–10). Higher SPAD values for *Quercus* species are generally associated with higher GDV classes. Differences are more pronounced for *Q. pubescens*. Red dots display the mean value.

Wilcoxon rank-sum test for the parameters showed highly significant differences for each individual parameter.

Nevertheless, GDV tends to be richer in species by two at the median. The overall number of different species identified in GDV is higher at 97 than in non-GDV at 83. The median coverage of phreatophytes for GDV is significantly higher at 63 % compared to 8 % for non-GDV.

Besides classical vegetation surveys, SPAD measurements were carried out to display differences between the vitality of two co-occurring

Quercus species in areas classified GDV and non-GDV (Fig. 4). The median for *Q. pubescens* is at 42.6 in GDV and significantly smaller at 29.2 in non-GDV. For *Q. ilex*, variances are less pronounced with SPAD values at 40.0 and 32.4 but still highly significant according to the Wilcoxon rank-sum test.

The significant differences between GDV or non-GDV locations derived from the probability map in terms of plant traits and SPAD represent a first validation of the presented workflow or the
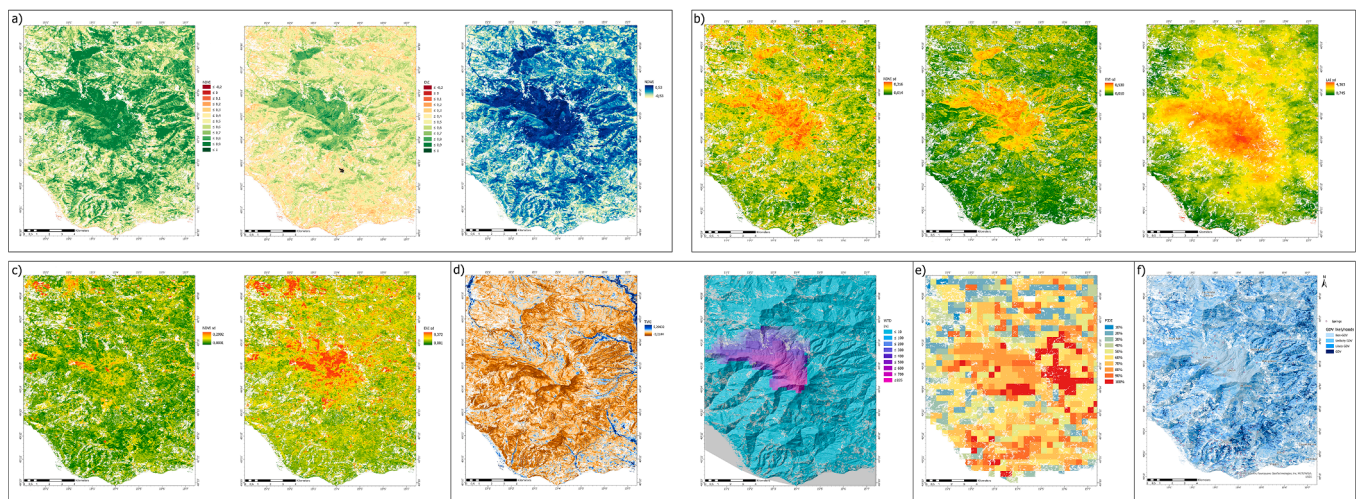
Fig. 5. Remote sensing and geodata products that were integrated in the ICUC classification of GDV likelihoods for the Mt. della Stella area. a) summarizes criterion 1 (NDVI, EVI, NDWI during the dry period). b) displays criterion 2 (seasonal changes of NDVI, EVI and LAI). c) shows criterion 3 (interannual changes of NDVI, EVI). d) integrates TWI and WTD as criterion 4. e) is criterion 5 (pIDE) and f) displays the final GDV likelihood map. All remote sensing indicators (NDVI, EVI, NDWI, LAI) display the mean over the period from 2017 to 2021.

classification.

4.2. Remote sensing, validation and calibration

All single parameters that were included in criterion 1–5 and in the classification are visualized in Fig. 5.

The GDV probability map got validated using results of in situ vegetation surveys, also focussing on calibration to derive class boundaries between GDV and non-GDV in order to create a GDV likelihood map. The criteria-based classification of plant traits allowed for independent labelling of vegetation field plots. According to the ecohydrological rule set, 41 % of the plots can be considered non-GDV, 18 % are unlikely GDV, 33 % likely GDV and 9 % GDV. These distributions were assigned to the GDV probability map in order to derive class boundaries for the GDV likelihoods. Therefore, non-GDV is represented in probability class 1–4, unlikely GDV account for class 5–6, likely GDV account for class 7–9 and GDV is summarized in class 10. For 62.7 % of the 116 vegetation plots the likelihoods derived from plant traits and classified by the ICUC match. In 32.7 % of the cases, higher likelihoods, and in 5.1 % lower likelihoods were assigned by the remote sensing classification. For 14.6 % of the plots non-GDVs were classified as GDVs (false positives), and only one GDV plot has been classified falsely as non-GDV (false negative).

The proportion of the arenaceous-conglomeratic HSU is much higher in non-GDV (17 %) than in GDV (2 %). Given the medium to high permeability of the HSU, which is consequently characterized by deeper groundwater flow (De Vita et al., 2018), it is likely that non-GDV is prevalent here. 80 % of all GDV is located on the arenaceous-marly-pelitic series which is characterized by low permeability of the rock mass favouring a surficial groundwater circulation into the regolith zone. GDV is less common in the arenaceous-conglomeratic HSU due to high permeable rocks where water infiltrates deeper and is less available to plants. However, GDV still can be found on the lower northern slope of Mount della Stella although the arenaceous-conglomeratic series

dominates. Since deep groundwater circulation is oriented towards the northern sector of Mount della Stella, many springs are located in this area (De Vita et al., 2018), therefore shallower local WTD as well as spring discharge favour the occurrence of some GDV.

Fig. 6 shows the most important land cover classes (Malinowski et al., 2020) in the study area and per GDV likelihood. With increasing groundwater dependency, the internal share of herbaceous vegetation decreases from 33 % to 5 % in favour of broadleaved trees where the share increases from 19 % to 39 %. Locations of GDV likelihoods in the landscape show proportional differences in terms of hydrogeology and landcover and thus serve as a further validation step against existing geodata.

A 2020 NDVI time series extracted for each vegetation plot shows differences in trend and value expression between GDV (likelihood classes 3 + 4) and non-GDV (likelihood classes 1 + 2) (Fig. 7). Overall, the median NDVI is higher in GDV (0.78) than in non-GDV (0.57) throughout the year. The mean alterations between both systems are twice as high (0.26) during the dry period than during the wet period (0.13). The interquartile range for each date is lower for GDV, especially within the dry period, which supports the idea of highly specialised vegetation ecosystems that only occur in a small range of favourable environmental conditions (Brown et al., 2009) and hence show similar spectral signals or properties within the study area.

The course of value expression in GDV and non-GDV is shifted. With onset of the dry period, NDVI values decrease for non-GDV, while GDV shows an opposite trend. Starting with the onset of the dry period in April a decrease in plant vitality is visible for non-GDV. As soon as the wet period starts, the NDVI increases drastically within non-GDV sites. This could be related to the high amount of scleromorphic species that show mechanisms of rapid water supply as soon as water is available (Ellenberg & Leuschner, 2010). Also, in GDV vitality increases but the response to the onset of precipitation seems delayed compared to non-GDV. The maximum NDVI within non-GDV is captured during the wet period. The maximum NDVI for GDV is recorded during the dry period.
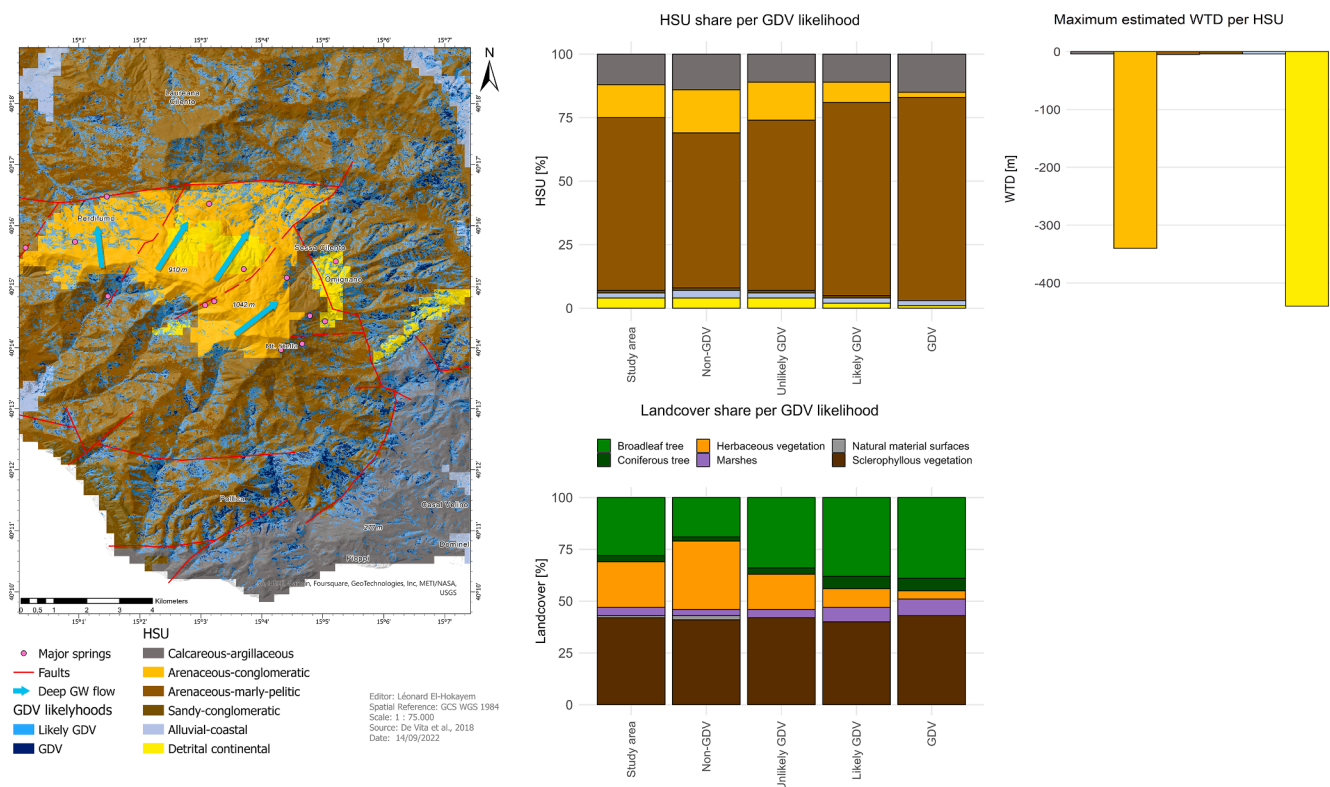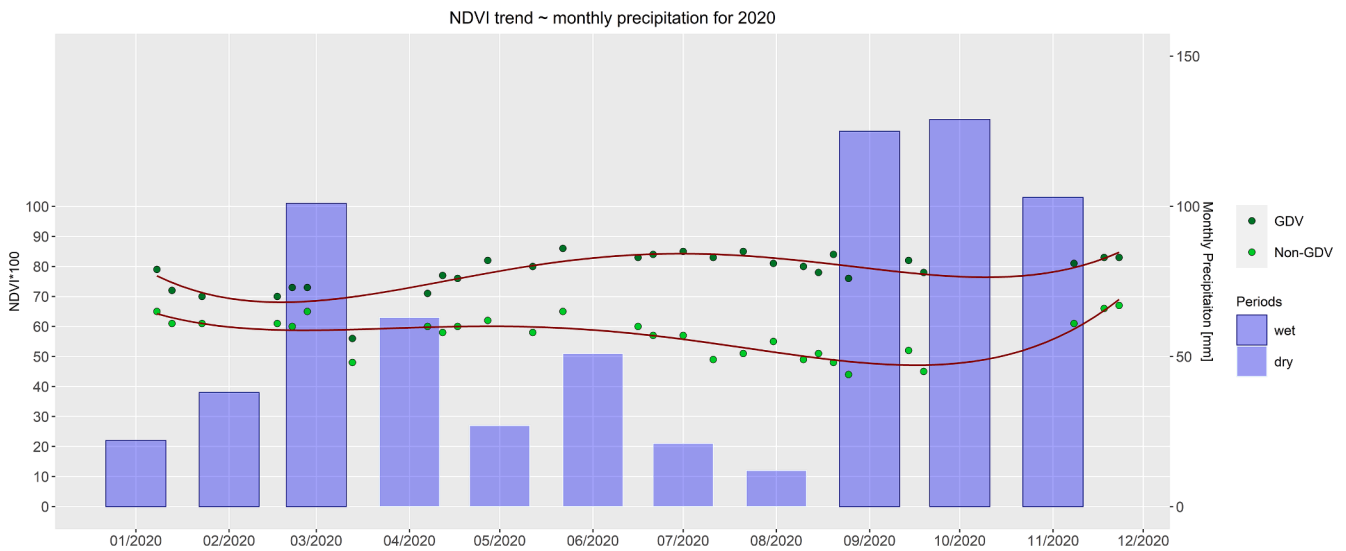

Fig. 6. Position of GDV likelihoods on the hydrogeological map of Mount della Stella, 1:75,000. Areal shares of likelihoods were compared in terms of HSU (with maximum estimated WTD) and land cover type in the study area.

NDVI trend ~ monthly precipitation for 2020

Fig. 7. Extracted NDVI values in GDV and non-GDV for 2020. NDVI got extracted for the 116 field plots. The modelled NDVI trend uses a fourth-degree polynomial function and was compared with mean monthly precipitation in the study area using CHIRPS precipitation data. Non-GDV and unlikely GDV as well as likely GDV and GDV were summarized as non-GDV and GDV respectively.

Overall, the progression of NDVI medians in GDV shows greater independence from precipitation, which strengthens the assumption of an external water source in this system and further validates the results from classification.
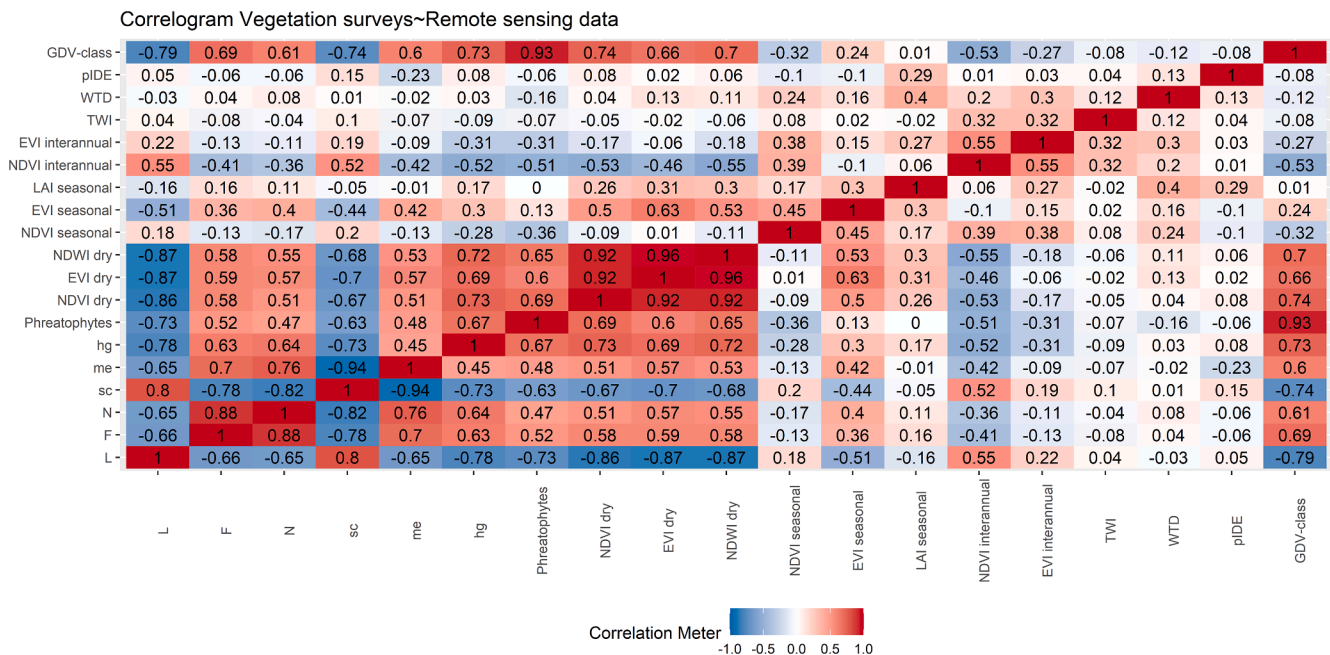
A correlation analysis between remote sensing criteria, in situ parameter and GDV classes from field work for the vegetation plot locations shows highest correlation between plant traits and mean indicator values during the dry period (Fig. 8). Overall, criteria relative to interannual and seasonal changes of NDVI, EVI and LAI show negligible to low correlations with in situ vegetation data. Also, no or negligible correlations occur between plant traits and pIDE, TWI or WTD. High positive correlations between remote sensing parameters and GDV classes are presented for mean NDVI, EVI and NDWI in the dry period, and moderate negative correlations for interannual changes of NDVI and

EVI or seasonal changes of NDVI. High intercorrelations between NDVI, EVI and NDWI within the dry period would allow to consider only NDVI as for criterion 1.

5. Discussion

5.1. Criteria and data

By using high-resolution S2-data to identify GDV in this study, low density and small range GDV that remained undetected in other studies (Doody et al., 2017; Páscoa et al., 2020) can be delineated. Furthermore, it can be assumed that the higher the resolution, the smaller the influence of mixed pixels becomes. Still, mixed pixels display a limitation of each remote sensing approach as they influence signals about vegetation

Correlogram Vegetation surveys~Remote sensing data

Fig. 8. Correlogram showing relationships between relevant vegetation parameters and remote sensing criteria used for the classification. GDV class respond to the likelihoods derived from the simple ecological rule set in the field.

coverage (Gou et al., 2015). Since S2-data are only available from 2015 onwards, long-term analyses of interannual changes as proposed by Doody et al. (2017) and Páscoa et al. (2020) are not possible. Long-term available satellite time series are likely to increase classification accuracy of climatic driven criteria, as relevant drought events may be excluded by only considering five years (Páscoa et al., 2020). Vegetation that uses groundwater outside of the studied period may not be identified. The high temporal resolution of the S2-data (5-days), on the other hand, supports the selection of suitable study periods during the dry period and for seasonal analyses, e.g., in semi-humid or humid biomes.

The presented methodological framework to identify local GDV in the Mediterranean can be understood as a combination and advancement of different approaches already tested in semi-arid and arid environments on local to continental scales. The five criteria that define the framework were selected based on the experience of previous studies (e. g., Barron et al., 2014; Doody et al., 2017; Gomes Marques et al., 2019; Gou et al., 2015; Páscoa et al., 2020). It is indicated that considering areas that remain green during dry periods (criterion 1) solely is insufficient in order to identify GDV. Vegetation that could be considered groundwater dependent according to that criterion, was found to also meet its water demand rather from soil moisture storage of thick soils in the AOI. It appears, that seasonal and interannual changes in plant vitality precise the final GDV map.

Criterion 2 aiming for seasonal changes in vitality may ignore deciduous GDV due to seasonal growing patterns and further classify evergreen vegetation that is not groundwater dependent as GDV (Barron et al., 2014).

Criterion 3 can be susceptible to fires and deforestation. On the other hand, criterion 3 highlights non-GDV due to lower vitality in particular dry years (2017) compared to more wet years (2018), which was found to be rather dependent on precipitation. However, pixels that show high moisture or vitality during a prolonged dry period as well as low seasonal and interannual changes, are likely to be groundwater dependent. Implementation of all three remote sensing criteria as introduced by Gou et al. (2015) and applied by Liu et al. (2021) is necessary in order to account for the typical phenology of different vegetation classes (e.g., evergreen vs deciduous) present in the study area. Nevertheless, independent classification runs for each land cover class or standardized NDVI timeseries (Páscoa et al., 2020) could also help to improve the accuracy in general.

For criterion 4 the spatial resolution of the WTD dataset allowed the classification as non-GDV for certain areas on Mount della Stella and its northern slopes, however, it was not helpful for high spatially variable classification at lower altitudes, as the WTD was below 4 m for 75 % of the territory and occurrence of phreatophytes and hence formation of GDV is possible. Results from TWI are limited to pinpoint locations of water accumulation in general and are no clear indicator for access of plants to groundwater.

As proposed by Doody et al. (2017), pIDE displays an easy criterion to address whether a system is inflow dependent or not. However, criterion 5 accounts for inflow in general and not for groundwater inflow solely, which can be a problem in regions with a high percentage of precipitation water supplied to surface runoff. The resolution of the precipitation data (0.05°) and also of the final pIDE product (500 m) is too coarse to meet the requirements of locally observed high spatial variability of GDV. Still, regional distribution of pIDE resembles patterns observed for plant vitality during the dry period. Nevertheless, for global approaches pIDE may display a good possibility to include climate data.

The integration of existing geodata from different sources on top of remote sensing analyses provides a more holistic approach to map GDV as it includes geographical site factors. Yet, local integration is limited by spatial and temporal resolution of datasets compared to remote sensing data as the results of the correlation show. The transferability to other areas and to larger scale levels still needs to be tested. Ground data derived from this study can be used as training data for supervised classification. Classification and Regression Trees (CART) offers the opportunity to identify relevant criteria and thresholds and hence holds the potential to transfer results to a larger area (Breimann et al., 1984. However, the concept can only be applied if the study area shows a well-defined seasonality of precipitation.

The specific plants traits recorded in the field hint only to groundwater dependency, as they are not able to actually confirm the presence of accessible groundwater as e.g., stable isotope analysis of plant water is able to (Jones et al., 2020). Differences in height, leaf anatomy and growth form between facultative phreatophytes growing as GDV or non-GDV show that identification of species alone is not sufficient though (Box et al., 2022). Accordingly, the occurrence of facultative phreatophytes hints to possible GDV but is not a fully proof of groundwater uptake. To overcome this uncertainty, including moisture value of non-phreatophyte species to the ecological rule set helps to reinforce the assumptions when data on rooting depth or WTD are not available.

Comprehensive vegetation surveys combined with in situ measurements of photosynthetic activity enhance the validation quality as they provide more information on vegetation than phreatophyte or land cover maps do. On the other hand, they are just punctual and complicate areal validation, which was overcome by also including commonly used data as for land cover or hydrogeology (e.g., Gou et al., 2015; Münch & Conrad, 2007).

5.2. GDV likelihood classification

The selected ICUC confirmed locations of GDV in the landscape that were conducted previously in similar studies and hence underpins its ability to GDV detection at the local scale. The likelihood map indicates that GDV is located in catchments with low hierarchical order where shallower groundwater circulation occurs in the regolith zone, and further represents the local morphology, topography, geology and runoff patterns (De Vita et al., 2018). GDV is often found near or along major faults, as stated in other studies (Doody et al., 2017; Münch & Conrad, 2007). This is related to rock fracturing and topography, which favour the accumulation and storage of water, or the emersion of deeper groundwater in springs due to the hydrogeological barrier effect (Doody et al., 2017).

Discrepancies in the assessment of groundwater dependence for criteria 1–3 along the northern slopes of Monte della Stella (arenaceous-conglomeratic complex) in terms of high vitality and moisture during the dry season, but secondly higher seasonal and interannual changes in vitality were observed. Knowing the high water retention properties and associated high storage of soil water in thick, volcanic soils (Napolitano et al., 2016; Mileti et al., 2017) combined with higher precipitation amounts at higher altitudes and, on the other hand, deep groundwater circulation at this part of the study area, the occurrence of a dense, deciduous, non-groundwater-dependent *C. sativa* forest endorses the classification results. These local edaphic characteristics provoke an exception in the presumed signals or behaviour of non-GDV during prolonged dry periods (criterion 1). However, *C. sativa* does not use groundwater and is adapted to drought stress, which favours the idea of *C. sativa* forests forming non-GDV mainly (Martínez-Sancho et al., 2017). Nevertheless, considering only vitality during the dry period would have led to misclassification as GDV and combination of several remote sensing criteria and geodata is necessary to enable a more robust and reliable classification.

Contrary to observations indicating that primary productivity of plants peaks during the wet season (e.g., Aronson & Shmida, 1992), the vitality (median NDVI) for GDV in this study is highest during the prolonged dry period. GDV may play a unique role here, as water availability is decoupled from current precipitation.

Significant variances between vegetation surveys of GDV and non-GDV for moisture, reaction and nitrogen are likely related to groundwater access in the study area, since other factors like: soil types, precipitation or temperature show a quite homogeneous spatial distribution (Killroy et al., 2008; Romano et al., 2018). A study by Casciello et al.

(1995) proved ranging pH value of groundwater samples between 6.3 and 8.9 in the AOI. Since the pH value of uncontaminated groundwater is higher than precipitation water, higher median reaction (R) values in GDV that account for more neutral to basic conditions are likely related to a higher groundwater contribution, as the water is classified as calcium-magnesium-bicarbonate (Casciello et al., 1995). While in non-GDV, lower values indicate that the vegetation is fed by precipitation water mostly (Killroy et al., 2008). Whereas, higher moisture values for GDV are likely to be directly associated with shallower and long-lasting groundwater levels and hence groundwater uptake or access by vegetation (Casciello et al., 1995). Differences in species richness indicate GDV to be richer in plant diversity and hence underpin the point that GDEs form biodiversity hotspots and habitats for threatened invertebrates, vertebrates as well as vascular plants, and are furthermore protectable systems (Brown et al., 2009).

Areas that were identified as GDV in the study area can contribute to the development of adapted water management methods and designation of systems worthy of protection or conservation within the National park area. As multiple ecosystems in semi-arid regions suffer from stress by increasing pressures of climate, land use and population change (Gou et al., 2015), locations of GDV help to determine extent or restrictions relative to the abstraction of groundwater. The local identification of GDV, however, is important in order to understand nature and location-dependency of these systems and thus delineate possible regions where even small changes in groundwater levels affect the survival of GDV (Eamus et al., 2006). In the Mount della Stella area this accounts for GDV located near settlements (especially tourism hotspots at the coast), cultivated areas and areas with a high density of wells and water reservoirs, while the whole area can be considered a climate change hotspot respectively (Ducroqc, 2016).

6. Conclusion

The framework developed in this study for identification of GDV in a Mediterranean environment can be understood as a step towards the creation of a harmonized, up-to-date GDV map for the Mediterranean biome. The classification results of the individual parameters or criteria illustrate that a focus solely on identification of areas that remain green and wet during the dry period (NDVI, NDWI, EVI) is not sufficient. Instead, seasonal and interannual changes of vitality (NDVI, EVI) as well as hydrogeological parameters such as TWI and WTD should be taken in account to ensure a robust and valid concept. Statistical analysis of 116 vegetation surveys showed significant differences between GDV and non-GDV in terms of plant traits and phreatophyte coverage. The relative leaf chlorophyll content derived from 100 SPAD measurements was higher for both observed *Quercus* species in GDV. It has been shown that pixels classified as GDV occur more frequently in broadleaf and coniferous forests and HSU with surficial groundwater circulation, which is typical of low permeability terrains. An ecological rule set derived from botanical field mapping was further suitable to calibrate four GDV likelihood classes. The problem of upscaling this localised knowledge to allow larger-scale GDV mapping is commonly recognised and will be tested in future studies. Nevertheless, local results received in this study provide already a valuable source for decision makers inside the national park area in order to apply sustainable groundwater management strategies.

CRediT authorship contribution statement

Léonard El-Hokayem: Conceptualization, Methodology, Software, Validation, Writing – original draft, Visualization. **Pantaleone De Vita:** Validation, Resources, Writing – review & editing. **Christopher Conrad:** Conceptualization, Resources, Writing – review & editing, Supervision.

Declaration of Competing Interest

The authors declare that they have no known competing financial interests or personal relationships that could have appeared to influence the work reported in this paper.

Data availability

Data will be made available on request.

References

Akasheh, O.Z., Neale, C.M.U., Jayanthi, H., 2008. Detailed mapping of riparian vegetation in the middle Rio Grande River using high-resolution multi-spectral airborne remote sensing. J. Arid Environ. 72, 1734–1744. https://doi.org/10.1016/j.jaridenv.2008.03.014.

Al-doski, J., Mansorl, S.B., Shafri, H.Z.M., 2013. Image classification in remote sensing. J. Environ. Earth Sci. 3 (10), 141–147.

Aronson, J., Shmida, A., 1992. Plant species diversity along a Mediterranean-desert gradient and its correlation with interannual rainfall fluctuations. J. Arid Environ. 23 (3), 235–247. https://doi.org/10.1016/S0140-1963(18)30513-5.

Barron, O.V., Emelyanova, I., Van Niel, T.G., Pollock, D., Hodgson, G., 2014. Mapping groundwater-dependent ecosystems using remote sensing measures of vegetation and moisture dynamics. Hydrol. Processes 28, 372–385. https://doi.org/10.1002/hyp.9609.

Beck, H.E., Zimmermann, N.E., McVicar, T.R., Vergopolan, N., Berg, A., Wood, E.F., 2018. Present and future Köppen Geiger climate classification maps at 1-km resolution. Scientific Data 5, 180214. https://doi.org/10.1038/sdata.2018.214.

Beven, K.J., Kirkby, M.J., 1979. A physically based, variable contributing area model of basin hydrology. Hydrol. Sci. Bull. 24, 43–69. https://doi.org/10.1080/02626667909491834.

Box, J.B., Leiper, I., Nano, C., Stokeld, D., Jobson, P., Tomlinson, A., Cobban, D., Bond, T., Randall, D., Box, P., 2022. Mapping terrestrial groundwater-dependent ecosystems in arid Australia using Landsat-8 time-series data and singular value decomposition. Remote Sens. Ecol. Conserv. 8 (4), 464–476. https://doi.org/10.1002/rse2.254.

Breimann, L., Friedman, J., Olshen, R., Stone, C.J., 1984. Classification and Regression Trees. Wadsworth, Belmont, CA.

Brown, J., Wyers, A., Bach, L., Aldous, A., 2009. Groundwater dependent biodiversity and associated threats: a statewide screening methodology and spatial assessment of Oregon. Nat. Conserv. 81.

Regione Campania, 2004. Carta Tecnica Numerica Regionale (1:5000 scale). Elements No.: 503052,503053, 503063, 503091, 503092, 503093, 503094, 503102, 503104, 503131, 503132, 503133, 503134, 503143, 503144, 519011, 519012, 519013, 519014, 519023, 519024. Progetto Cofinanziato dal P.O.R. Campania 2000/6. Misura 6.2.

Casciello, C., De Vita, P., Stanzione, D., Vallario, A., 1995. Idrogeologia e Idrogeochimica del Mount della Stella (Cilento – Campania Meridionale). Quaderni di Geologia Applicata 2, 327–334.

De Vita, P., Allocca, V., Celico, F., Fabbrocino, S., Mattia, C., Monacelli, G., Musili, I., Piscopo, V., Scalise, A.R., Summa, G., Tranfaglia, G., Pietro, C., 2018. Hydrogeology of continental southern Italy. J. Maps 14 (2), 230–241. https://doi.org/10.1080/17445647.2018.1454352.

Doody, T.M., Barron, O.V., Dowsley, K., Emelyanova, I., Fawcett, J., Overton, I.C., Pritchard, J.L., Van Dijk, A., Warren, G., 2017. Continental mapping of groundwater dependent ecosystems: a methodological framework to integrate diverse data and expert opinion. J. Hydrol.: Regional Stud. 10, 61–81. https://doi.org/10.1016/j.ejrh.2017.01.003.

Ducroqc, V., 2016. Climate change in the Mediterranean region. In: Thiébault, S., Moatti, J.-.-P. (Eds.), The Mediterranean Region Under Climate Change. IRD Éditions, pp. 71–104.

Duda, T., Canty, M., 2002. Unsupervised classification of satellite imagery: choosing a good algorithm. Int. J. Remote Sens. 23 (11), 2193–2212. https://doi.org/10.1080/01431160110078467.

Eamus, D., Froend, R., Loomes, R., Hose, G., Murray, B., 2006. A functional methodology for determining the groundwater regime needed to maintain the health of groundwater-dependent vegetation. Austral. J. Bot. 54 (2), 97–114. https://doi.org/10.1071/BT05031.

Eamus, D., Zolfaghar, S., Villalobos-Vega, E., Cleverly, J., Huete, A., 2015. Groundwater-dependent ecosystems: recent insights from satellite and field-based studies. Hydrol. Earth Syst. Sci. 19, 4229–4256. https://doi.org/10.5194/hess-19-4229-2015.

Eamus, D., Fu, B., Springer, A.E., Stevens, L.E., 2016. Groundwater Dependent Ecosystems: Classification, Identification Techniques and Threats. In: Jakeman, A.J., Barreteau, O., Hunt, R.J., Rinaudo, J.-D., Ross, A. (Eds.), Integrated Groundwater Management. Springer, pp. 313–346. https://doi.org/10.1007/978-3-319-23576-9_13.

European Commision (EC), 2007. European Commission DG Environment, LIFE and Europe's wetlands, Restoring a vital ecosystem. LIFE III EC, doi:10.2779/22840.

Ellenberg, H., 1974. Zeigerwerte der Gefäßpflanzen Mitteleuropas. Scripta Geobotanica 9, 1–97.

Ellenberg, H., Leuschner, C., 2010. Vegetation Mitteleuropas mit den Alpen. Ulmer.

ESA, 2021. Copernicus Sentinel-2 data. ESA.

ESRI:https://desktop.arcgis.com/en/arcmap/10.3/tools/spatial-analyst-toolbox/iso-cluster-unsupervised-classification.htm, last access: 17 September.2022.

European Environment Agency (EEA), 2017. EUNIS habitat classification 2017 (Revised forest heathland scrub tundra). EEA.

Evaristo, J., McDonnell, J.J., 2017. Prevalence and magnitude of groundwater use by vegetation: a global stable isotope meta-analysis. Sci. Rep. 7, 44110. https://doi.org/10.1038/srep44110.

Funk, C., Peterson, P., Landsfeld, M., Pedreros, D., Verdin, J., Shukla, S., Husak, G., Rowland, J., Harrison, L., Hoell, A., Michaelsen, J., 2015. The climate hazards infrared precipitation with stations—a new environmental record for monitoring extremes. Sci. Data 2, 150066. https://doi.org/10.1038/sdata.2015.66.

Gao, B., 1996. NDWI—A normalized difference water index for remote sensing of vegetation liquid water from space. Remote Sens. Environ. 58 (3), 257–266. https://doi.org/10.1016/S0034-4257(96)00067-3.

Gomes Marques, I., Nascimento, J., Cardoso, R.M., Miguéns, F., Condesso de Melo, M.T., Soares, P.M.M., Gouveia, C.M., Kurz Besson, C., 2019. Mapping the suitability of groundwater-dependent vegetation in a semi-arid Mediterranean area. Hydrol. Earth. Syst. Sci. 23, 3525–3552. https://doi.org/10.5194/hess-23-3525-2019.

Gou, S., Gonzales, S., Miller, G.R., 2015. Mapping potential groundwater-dependent ecosystems for sustainable management. Groundwater 53 (1), 99–110. https://doi.org/10.1111/gwat.12169.

Green, S. & Cooper, R., 2016. South-East of Falmouth rMCZ Post-survey Site Report. Technical Report. Department for Environment, Food and Rural Affairs.

Hoogland, T., Heuvelink, G.B.M., Knotters, M., 2010. Mapping water-table depths over time to access desiccation of groundwater-dependent ecosystems in the Netherlands. Wetlands 30, 137–147. https://doi.org/10.1007/s13157-009-0011-4.

Huete, A., Didan, K., Miura, T., Rodriguez, E., Gao, X., Ferreira, L., 2002. Overview of the radiometric and biophysical performance of the MODIS vegetation indices. Remote Sens. Environ. 83 (1), 195–213. https://doi.org/10.1016/S0034-4257(02)00096-2.

Jones, C., Stanton, D., Hamer, N., Denner, S., Singh, K., Flook, S., Dyring, M., 2020. Field investigation of potential terrestrial groundwater-dependent ecosystems within Australia's Great Artesian Basin. Hydrogeol. J. 28, 237–261. https://doi.org/10.1007/s10040-019-02081-1.

Killroy, G., Dunne, F., Ryan, J., O'Connor, Á., Daly, D., Craig, M., Coxon, C., Johnston, P., Moe, H., 2008. A Framework for the Assessment of Groundwater-Dependent Terrestrial Ecosystems under the Water Framework Directive. Available at. Environmental Protection Agency, Wexford.

Liu, C., Liu, H., Yu, Y., Zhao, W., Zhang, Z., Guo, L., Yetemen, O., 2021. Mapping groundwater-dependent ecosystems in arid Central Asia: implications for controlling regional land degradation. Sci. Total Environ. 797 https://doi.org/10.1016/j.scitotenv.2021.149027.

Lv, J., Wang, X.S., Zhou, Y., Qian, K., Wan, L., Eamus, D., Tao, Z., 2012. Groundwater-dependent distribution of vegetation in Hailiutu River catchment, a semi-arid region in China. Ecohydrology 6, 142–149. https://doi.org/10.1002/eco.1254.

Malinowski, R., Lewinski, S., Rybicki, M., Gromny, E., Jenerowicz, M., Krupinski, M., Nowakowski, A., Wojtkowski, C., Krupinski, M., Krätzschmar, E., Schauer, P., 2020. Automated Production of a Land Cover/ Use Map of Europe Based on Sentinel-2 Imagery. Remote sens. 12, 3523. https://doi.org/10.3390/rs12213523.

Marínez-Santos, P., Díaz-Alcaide, S., De la Hera-Portillo, A., Gómez-Escalonilla, V., 2021. Mapping groundwater-dependent ecosystems by means of multi-layer supervised classification. J. Hydrol. https://doi.org/10.1016/j.jhydrol.2021.126873.

Greenberg, J.A., 2020. spatial.tools: R functions for Working with Spatial Data. R package version 1.6.2.

Martínez-Sancho, E., Vásconez Navas, L.K., Seidel, H., Dorado-Liñán, Menzel. A., 2017. Responses of Contrasting Tree Functional Types to Air Warming and Drought. Forests, 8, 450, doi:10.3390/f8110450.

Maxey, G.B., 1964. Hydrostratigraphic units. J. Hydrol. 2, 124–129. https://doi.org/10.1016/0022-1694(64)90023-X.

Meinzer, O.E., 1927. Plants as indicators of ground water. USGS Water-Supply Paper, 577.

Mileti, F.A., Vingiani, S., Manna, P., Langella, G., Terribile, F., 2017. An integrated approach to studying the genesis of andic soils in Italian nonvolcanic mountain ecosystems. Catena 159, 35–50. https://doi.org/10.1016/j.catena.2017.07.022.

Münch, Z., Conrad, J., 2007. Remote sensing and GIS based determination of groundwater dependent ecosystems in the Western Cape, South Africa. Hydrogeol. J. 15, 19–28. https://doi.org/10.1007/s10040-006-0125-1.

Napolitano, E., Fusco, F., Baum, R.L., Godt, J.W., De Vita, P., 2016. Effect of antecedent-hydrological conditions on rainfall triggering of debris flows in ash-fall pyroclastic mantled slopes of Campania (southern Italy). Landslides 13, 967–983. https://doi.org/10.1007/s10346-015-0647-5.

Páscoa, P., Gouveia, C.M., Kurz-Besson, C., 2020. A simple method to identify potential groundwater-dependent vegetation using NDVI MODIS. Forests 11, 147. https://doi.org/10.3390/f11020147.

Pasquarella, V.J., Holden, C.E., Kaufman, L., Woodcock, C.E., 2016. From imagery to ecology: leveraging time series of all available Landsat observations to map and monitor ecosystem state and dynamics. Remote Sens. Ecol. Conserv. 2, 152–170. https://doi.org/10.1002/rse2.24.

Pérez Hoyos, I.C., Krakauer, N.Y., Khanbilvardi, R., Armstrong, R.A., 2016. A review of advances in the identification and characterization of groundwater dependent ecosystems using geospatial technologies. Geosciences 6, 17. https://doi.org/10.3390/geosciences6020017.

Pignatti, S., Menegoni, P., Pietrosanti, S., 2005. Biondicazione attraverso le piante vascolari. Valori di indicazione secondo Ellenberg (Zeigerwerte) per le specie della Flora d'Italia. Braun-Blanquetia 39, 1–97.

Pignatti, S., 1982. Flora D'Italia. Edagricole.

Ranghetti, L., Boschetto, F., Nutini, F., Busetto, L., 2020. sen2r: An R toolbox for automatically downloading and preprocessing Sentinel-2 satellite data. Comput. Geosci. 139, 104473 https://doi.org/10.1016/j.cageo.2020.104473.

Richardson, A.D., Duigan, S.P., Berlyn, G.P., 2002. An evaluation of non-invasive methods to estimate chlorophyll content. New Phytol. 153 (1), 185–194. https://doi.org/10.1046/j.0028-646X.2001.00289.x.

Romano, N., Nasta, P., Bogena, H., De Vita, P., Stellato, L., Vereecken, H., 2018. Monitoring hydrological processes for land and water resources management in a Mediterranean ecosystem: the Alento River catchment observatory. Vadose Zone J. 17, 180042 https://doi.org/10.2136/vzj2018.03.0042.

Rouse, J.W., Haas, R.H., Schell, J.A., Deering, D.W. & Harlan, J.C., 1974. Monitoring the vernal advancement of retrogradiation of natural vegetation. NASA/GSFC, Type III, Final Report, 371.

Running, S., Mu, Q., Zhao, M., 2017. MOD16A3 MODIS/Terra Net Evapotranspiration Yearly L4 Global 500m SIN Grid (006) [Data set]. NASA EOSDIS Land Processes DAAC, doi:10.5067/MODIS/MOD16A3.006.

Selby, M.J., 1993. Hillslope Materials and Processes. Oxford University Press, p. 451.

Thomas, F.M., 2014. Ecology of Phreatophytes. In: Lüttge, U. (Ed.), Progress in Botany 75. Springer, pp. 335–375. https://doi.org/10.1007/978-3-642-38797-5_11.

Traxler, A., 1997. Handbuch des vegetationsökologischen Monitorings. Methoden, Praxis, angewandte Projekte Teil A: Methoden. Umweltbundesamt.

Tuel, A., Eltahir, E.A.B., 2020. Why is the mediterranean a climate change hot spot? J. Clim. 33 (14), 5829–5843. https://doi.org/10.1175/JCLI-D-19-0910.1.

Tweed, S.O., Leblanc, M., Webb, J.A., Lubczynski, M.W., 2007. Remote sensing and GIS for mapping groundwater recharge and discharge areas in salinity prone catchments, southeastern Australia. Hydrogeol. J. 15 (1), 75–96. https://doi.org/10.1007/s10040-006-0129-x.

Weiss, M., Baret, F., 2016. S2ToolBox Level 2 products: LAI, FAPAR, FCOVER v.1.1. INRA.